



## Original Article

# Fabrication of high performance energy storage EDLC device from proton conducting methylcellulose: dextran polymer blend electrolytes

Shujahadeen B. Aziz<sup>a,b,\*</sup>, M.A. Brza<sup>a,c</sup>, Kuldeep Mishra<sup>d</sup>, M.H. Hamsan<sup>e</sup>, Wrya O. Karim<sup>f</sup>, Ranjdar M. Abdullah<sup>a</sup>, M.F.Z. Kadir<sup>e</sup>, Rebar T. Abdulwahid<sup>a,g</sup>

<sup>a</sup> Advanced Polymeric Materials Research Lab., Department of Physics, College of Science, University of Sulaimani, Qlyasan Street, Sulaimani, Kurdistan Regional Government, Iraq

<sup>b</sup> Komar Research Center (KRC), Komar University of Science and Technology, Sulaimani, 46001, Kurdistan Regional Government, Iraq

<sup>c</sup> Department of Manufacturing and Materials Engineering, Faculty of Engineering, International Islamic University of Malaysia, Kuala Lumpur, Gombak, Malaysia

<sup>d</sup> Department of Physics and Materials Science, Jaypee University, Anoopshahr, India

<sup>e</sup> Centre for Foundation Studies in Science, University of Malaya, Kuala Lumpur, Malaysia

<sup>f</sup> Department of Chemistry, College of Science, University of Sulaimani, Qlyasan Street, Sulaimani, Kurdistan Regional Government, Iraq

<sup>g</sup> Department of Physics, College of Education, University of Sulaimani, Old Campus, Sulaimani, Kurdistan Regional Government, Iraq

## ARTICLE INFO

## Article history:

Received 10 August 2019

Accepted 17 November 2019

Available online xxx

## Keywords:

Polymer blend electrolytes

XRD and FTIR study

Impedance spectroscopy

TNM and LSV analysis

Cyclic voltammetry

EDLC

## ABSTRACT

This paper reports Methylcellulose:Dextran (MC:Dex) polymer blend based electrolyte system with  $\text{NH}_4\text{I}$  salt for electrical double layer capacitor (EDLC) application. The structural and electrochemical properties of the electrolyte systems were investigated using X-ray diffraction (XRD), Fourier transformed infra-red (FTIR) spectroscopy, Field emission scanning electron microscope (FESEM), impedance spectroscopy, transference number measurement (TNM) and linear sweep voltammetry (LSV). The FTIR studies revealed the complexation between MC:Dex polymer blend and  $\text{NH}_4\text{I}$  salt. The reduction in the crystallinity of MC:Dex polymer blend with the increasing salt concentration was observed in XRD analysis. The electrolyte system was observed to be predominantly ionic in nature. The electrolyte composition with 40 wt.% of  $\text{NH}_4\text{I}$  showed the maximum ionic conductivity as  $1.12 \times 10^{-3} \text{ S/cm}$  with electrochemical stability window of 1.27 V. The highest conducting composition of the electrolyte system was used to prepare EDLC with activated carbon electrodes. The EDLC exhibited initial specific capacitance as 79 F/g, energy density as 8.81 Wh/kg and power density as 1111.1 W/kg at a current density of 0.2 mA/cm<sup>2</sup>.

© 2019 The Authors. Published by Elsevier B.V. This is an open access article under the CC BY-NC-ND license (<http://creativecommons.org/licenses/by-nc-nd/4.0/>).

\* Corresponding author.

E-mails: [shujaadeen78@yahoo.com](mailto:shujaadeen78@yahoo.com), [shujahadeenaziz@gmail.com](mailto:shujahadeenaziz@gmail.com) (S.B. Aziz).

<https://doi.org/10.1016/j.jmrt.2019.11.042>

2238-7854/© 2019 The Authors. Published by Elsevier B.V. This is an open access article under the CC BY-NC-ND license (<http://creativecommons.org/licenses/by-nc-nd/4.0/>).

## 1. Introduction

Capacitors are electrical energy storage devices that have been used in a wide range of applications, such as our daily use electronic devices, transportation means, medical utilities and defense related systems [1]. Nowadays, electrical double layer capacitors (EDLCs), also referred to as supercapacitors, ultracapacitors and pseudocapacitors utilize different choices of electrolyte materials and carbon electrodes. These devices are in competition with other types of power sources, especially rechargeable batteries [2]. When choosing a desirable EDLC device, several parameters are needed to be taken into consideration, such as specific energy/power, charge-discharge cycle life and satisfactory safety [1]. The performance of EDLC can be improved either by the modification of the electrodes or materials mediated between the electrodes. Recent studies have revealed that polymer electrolytes (SPEs) are considered as the best promising candidates in the electrochemical devices, owing to their common benefits, such as solvent free, leakage-free, transparency, lightweight, elasticity, easy handling, easily forming thin films, good conductivity, and wide electrochemical windows in comparison to commercial liquid electrolyte counterparts [3,4]. To the best of our knowledge, the polymers that used in polymer electrolytes of energy storage devices as host materials are categorized into two main types; natural and synthetic polymers [5]. On one hand, most of the synthetic polymers are non-biodegradable, such as polyethylene oxide, polymethyl methacrylate, polyvinyl chloride, polycarbonate and polyacrylonitrile [6]. However, there is an existence of non-biodegradable synthetic polymers causing the depletion of petroleum resources and increase the disposal problems [7]. On the other hand, biopolymers can be used as the host polymer in energy storage devices, which minimize plastic waste pollution on the environment. It is apparent that the biopolymers are obtained from natural resources and offering unique characteristics, such as cheapness, compatibility with various solvents, abundance and ease of film forming [8–11]. For instance, starch, cellulose, chitosan, dextran and carrageenan are the most common biopolymers used in polymer electrolyte explorations [12–16]. Natural biopolymers tend to decay naturally, whereas synthetic polymers are relatively indestructible [7,17]. The most abundant organic polymer in nature is cellulose. It is accordingly regarded as an absolutely favorable renewable resource [18]. Recently, cellulose materials as a natural polymer are considered as alternatives to organic materials and may replace the petrochemical polymers [19]. Among these natural polymer materials, methyl cellulose (MC) is an abundant, cheap, and environmentally friendly class. As a cellulose derivative, MC is obtained from methylation of alkali cellulose and characterized by its biodegradability and satisfactory film forming properties, such as transparency and superior mechanical and electrical properties [7]. Modification of biopolymer, for example, methylcellulose with-1,4 glycosidic bond has been carried out via the introduction of methyl chloride or dimethyl sulfate to alkali based cellulose [20]. As it is known, certain ions can form a complex with oxygen containing functional groups of the polymer host by dative bond. MC contains functional groups, for instance hydroxyl, glycosidic bond and methoxy

groups possess lone pair electrons, which are responsible for the ionic conduction [21,22]. This natural polymer has plausible solubility mechanical, thermal, and chemical stabilities as well as the excellent film-forming character, making the MC suitable for exceptional purposes [23]. Moreover, it is an amorphous polymer that has a relatively high glass transition temperature ( $T_g$ ), ranging from 184 to 200 °C [22]. Likewise, dextran is another non-toxic and biodegradable polysaccharide. It can be obtained from the reproduction of bacteria *Leuconostoc mesenteroides*. This polysaccharide enriches in lone pair electron on heteroatoms, such as oxygen, which is necessary for dissolving inorganic salts [16]. It is well reported that polymer blend methodology provides more sites for ionic conduction [24]. It is emphasized that polymer blending methodology is a proper way for lowering the degree of crystallinity and thus increasing glass transition [25,26].

The downsizing trend of electronic device has motivated researchers to spend much effort towards EDLC devices [3]. EDLC can be used as an alternative to conventional batteries. Various materials can be employed as electrodes in these electrochemical devices [27,28]. The energy storage mechanism of EDLC involves non-Faradaic reaction, where ions form double-layer on its carbon-based electrodes [29]. Many advantages can be acquired from such device, such as higher power density, better thermal stability, longer life cycle, higher reversibility, cost-effective, fast charge-discharge rate, safe and simple fabrication techniques than Faradaic capacitor or pseudocapacitor [30–32]. Nowadays, activated carbon has been studied to be compatible with polymer electrolyte [33,34]. There are several favorable properties that make activated carbon preferable to be used in EDLC, such as high electrical conductivity, cost-effectiveness and excellent chemical stability as well as large surface area [35]. In addition to the device configuration, the electrode and electrolyte materials have a significant effect on the EDLC device performance. Although, there has been a great deal of work on manipulation of electrode materials, there has been little research on the electrolytes in supercapacitors. The key concepts of using electrolytes in supercapacitors are factors of determining electrochemical potential window, cycle life and safety [36].

In this work, firstly the electrical properties of methylcellulose:Dextran (MC:Dex) blend doped with ammonium iodide ( $\text{NH}_4\text{I}$ ) are analyzed. Later on, a relatively highest conducting electrolyte sample is used in EDLC device. The results showed that polymer blending based on natural resources can be used for EDLC device fabrication with a high performance.

## 2. Experimental method

### 2.1. Materials and sample preparation

Methyl cellulose (MC) and dextran (Dex) powders were used as raw materials, which are provided by Sigma Aldrich (Sigma-Aldrich, Kuala Lumpur, Malaysia). For the preparation of the MC:Dex blended polymer, 70 wt.% of MC and 30 wt.% of Dex were dissolved separately, each in 50 mL of distilled water at room temperature for 180 min. Subsequently, the solution was mixed and stirred for 4 h to obtain a homogeneous blending solution. Then, different amounts of ammonium iodide ( $\text{NH}_4\text{I}$ )

[CAS Number 12027-06-4, Molecular Weight = 144.94 g/mol] from 10 to 40 wt.% in steps of 10 were added separately to the MC:Dex blended solution with continuous stirring to obtain MC:Dex:NH<sub>4</sub>I electrolytes. The polymer blend electrolytes were coded as MCD0, MCD1, MCD2, MCD3, and MCD4 for MC:Dex incorporated with 0, 10, 20, 30, and 40 wt% of NH<sub>4</sub>I, respectively. After casting the solutions of constituents in the labeled Petri dishes (90 mm × 15 mm, Sigma-Aldrich, Kuala Lumpur, Malaysia), the solvent was allowed to evaporate at room temperature. Additional drying was induced by transferring the films to a desiccator. In this way, solvent-free electrolyte films were obtained.

## 2.2. Structural, impedance and morphological characterizations

X-ray diffraction (XRD) patterns were obtained for the samples using Empyrean X-ray diffractometer (PANalytical, Netherlands) with operating voltage and current of 40 kV and 40 mA, respectively. A beam of monochromatic CuK<sub>α</sub> X-ray of wavelength 1.5406 Å was used to irradiate the samples, where the glancing angles was in the range of  $5^\circ \leq 2\theta \leq 80^\circ$  with a step size of  $0.1^\circ$ . Fourier transforms Infrared (FTIR) spectroscopy measurements were performed using Spotlight 400 Perkin-Elmer spectrometer with a resolution of  $1\text{ cm}^{-1}$  ( $450\text{--}4000\text{ cm}^{-1}$ ). A Hitachi SU8220 FESEM (Tokyo, Japan) was utilized to investigate the surface morphology of the blend electrolyte films at 500× magnification. HIOKI 3532-50 LCR HiTESTER was employed to analyze electrical impedance spectroscopy (EIS) measurements of the samples (50 Hz to 5 MHz).

## 2.3. Transference number measurement (TNM) and linear sweep voltammetry (LSV)

V&A Instrument DP3003 digital DC power supply was employed to analyze ionic ( $t_{ion}$ ) and electronic ( $t_{el}$ ) transference number. The largest conducting electrolyte was located in a teflon holder with similar stainless steel electrodes. The cell was subjected to 0.20 V at room temperature. To investigate the electrolyte electrochemical stability, linear sweep voltammetry (LSV) method was employed as a measurement technique via Digi-IVY DY2300 potentiostat. The applied scan rate was  $100\text{ mV s}^{-1}$ . For this purpose, the electrolyte was located between two stainless steel of a teflon holder. Fig. 1 shows a schematic illustration of the stainless steel electrodes for both TNM and LSV analyses.

## 2.4. EDLC preparation

An amount of 0.25 g carbon black was combined with 3.25 g activated carbon with planetary ball miller before the mixture was poured in solution of 15 ml N-methyl pyrrolidone (NMP) and 0.50 g of polyvinylidene fluoride (PVdF). Black and thick solution was emerged upon dissolution. An aluminum foil was cleaned by acetone and flattened on glass surface. The solution was poured and spread on the foil by doctorblade technique. The electrodes were left in the oven for drying at  $60^\circ\text{C}$ . The dried electrodes were then placed in a desiccator for further drying. The electrode was cut into a small circle shape with area of  $2.01\text{ cm}^2$ . Electrolyte with the largest con-

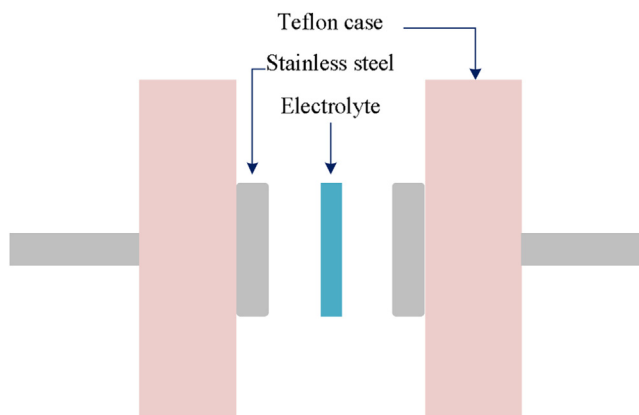


**Fig. 1 – Schematic illustration of the stainless steel electrodes for TNM and LSV study.**

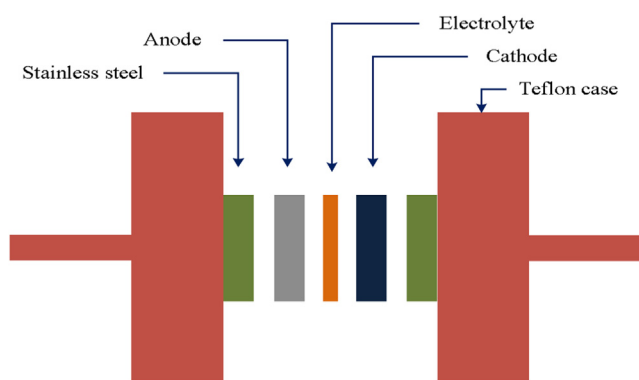


**Fig. 2 – Schematic illustration of the EDLC cell for charge-discharge measurement.**

ductivity was located between two activated carbon electrodes and packed in a CR2032 coin cell. The EDLC characteristic was verified by cyclic voltammetry (CV) analysis at a scan rate of  $10\text{ mV s}^{-1}$ . The EDLC charge-discharge profiles were tested by Neware battery cycler with a current density of  $0.2\text{ mA cm}^{-2}$ . Fig. 2 shows schematic illustration of the EDLC cell for the charge-discharge measurements.

## 3. Results and discussion

### 3.1. Structural and morphological study

Fig. 3(a–c) shows the X-ray patterns for the prepared MC:Dext films. It is well reported that MC host polymer has a unique peak at  $2\theta = 19\text{--}21^\circ$ , resulting from the intermolecular hydrogen bonding coupled with a short-distance order in the MC polymer chains [37–39]. Dextran is also known to have two broad peaks at  $2\theta = 18$  and  $23^\circ$  [16]. More interesting observation is that the XRD pattern of the MC:Dext system has only exhibited one concave peak [see Fig. 3(b)] in addition to some small peaks. These broad hollows indicate the domination of a certain feature of the MC:Dext blend composite, which is the complete amorphous structure [4,40]. Therefore, a great opportunity for decreasing crystallinity and subsequently enhancing conductivity can be the implementation of

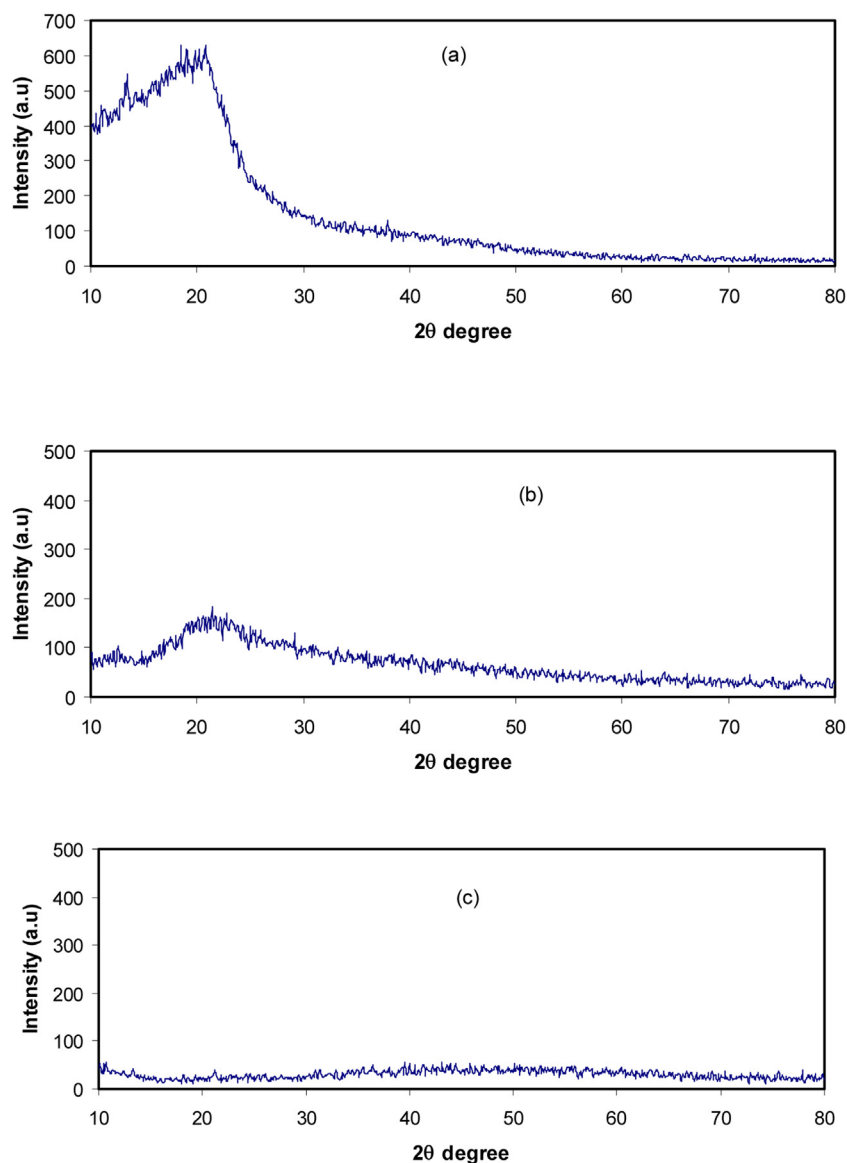


Fig. 3 – XRD pattern for (a) MCD0, (b) MCD2 and (c) MCD4 polymer electrolyte films.

polymer blending strategy. This approach involves mixing at least two structurally different kinds of polymers via interact through secondary forces with non-covalent bonding [41]. The XRD patterns for chosen blend electrolyte samples are shown in Fig. 3(b,c). It is obvious that with the addition of 20 wt.% of inorganic  $\text{NH}_4\text{I}$  salt into MC:Dext matrix, the hollow intensity of the MC:Dext was drastically lowered as shown in Fig. 3(b). This is an indication of lowering of crystalline region of the polymer blend and thus enhancing the amorphous phase [42]. From Fig. 3(c), it is clearly seen that an addition of 40 wt.% of  $\text{NH}_4\text{I}$  salt resulted in more broadened hollow. This finding shows that both peak widening and peak intensity lowering in diffractogram are reasonable evidence of the dominance of the amorphous region within the polymer system as anticipated.

It is documented that one can investigate the trend of conductivity of the electrolytes through the analysis of XRD pattern [43]. Upon the addition of the inorganic salt into the MC:Dext system, the degree of crystallinity has been reduced,

which can be related to the complex formation between polar groups of the polymer and the salt cations ( $\text{NH}_4^+$ ) through electrostatic interactions. Consequently, it caused to retard the ordering of the crystalline regions inside the polymer electrolyte through disrupting hydrogen bonding [44]. From Hodge et al.'s criterion, there is a correlation between the peak intensity and the degree of crystallinity, in which the change in intensity and particularly the peak broadening in the XRD pattern are considered to be indicators for the amorphous feature of the sample [45].

### 3.2. FTIR analysis

Fig. 4(a and b) exhibits the FTIR spectra of the pure MC:Dext and doped MC:Dext films in the regions of (a)  $400\text{ cm}^{-1}$  to  $2400\text{ cm}^{-1}$  and (b)  $2400\text{ cm}^{-1}$  to  $4000\text{ cm}^{-1}$ . It is known that to confirm the hydrogen bond formation within the polymer electrolytes based on MC:Dex films, one can use FTIR



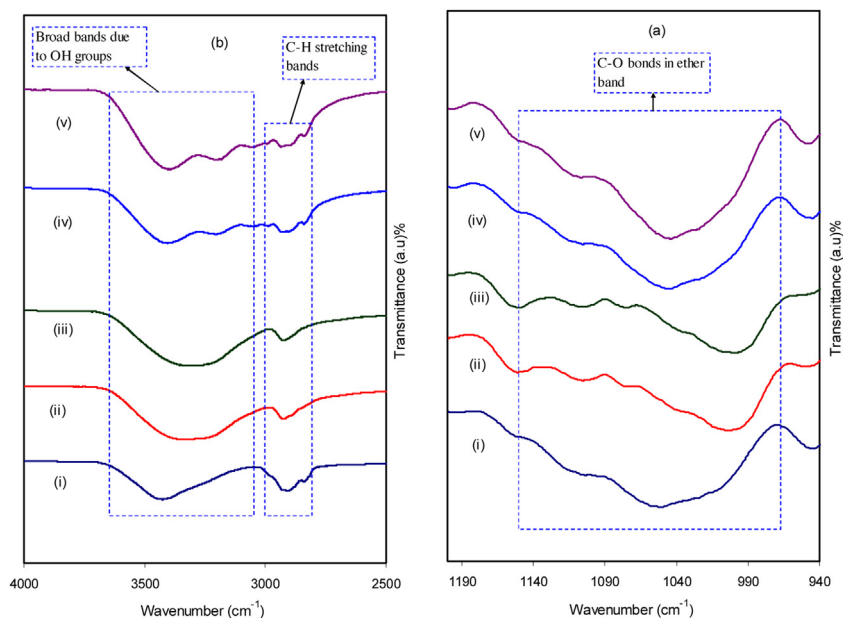


**Fig. 4 – FTIR spectra of (i) MC:Dext (pure film, MCD0), (ii) MCD1, (iii) MCD2, (iv) MCD3, and (v) MCD4 in the region (a) 940  $\text{cm}^{-1}$  to 1190  $\text{cm}^{-1}$ , and (b) 2500  $\text{cm}^{-1}$  to 4000  $\text{cm}^{-1}$ .**

spectroscopy. The principle of such technique is based on stretching vibration frequencies of the bonds, where each bond has a characteristic frequency [46]. As an example, the hydroxyl band observed for the pure MC:Dext system can be attributed to the wavenumber region 3447–3458  $\text{cm}^{-1}$ , though each band needs to be at 1066  $\text{cm}^{-1}$  and 1110  $\text{cm}^{-1}$  [47]. It is well-known that FTIR spectroscopy has been widely used in dealing with the formation of polymer blends. It provides insight into intermolecular interaction through the FTIR spectra analysis in terms of stretching and bending vibrations of bonds. In this report, FTIR analysis is used for the MC:Dext polymer blend electrolyte, wherein the presence of OH groups is shown from the appearance of broad band with a maximum at 3351  $\text{cm}^{-1}$  [48,49]. It is apparent that absorption bands centered at 3458  $\text{cm}^{-1}$  in both pure MC:Dext and doped MC:Dext electrolyte films can ascribed to the O–H stretching [50,51] and the band peaked at 2906  $\text{cm}^{-1}$  was attributed to C–H stretching in dextran [48,49]. More interesting observation was that the incorporation of  $\text{NH}_4\text{I}$  salt into MC:Dext caused a significant change in the bands intensity. This change in intensity is resulted strongly from the alterations in the macromolecular order. These bands in the spectra of the complexes may result from the extent of ordered structures [52]. It is evident from Fig. 4b that the hydroxyl band for the pure MC:Dext film has appeared in the form of a symmetric and homogeneous shoulder. On the other hand, for the blend electrolyte samples, a broad and asymmetric shoulder was seen. The wavenumber region from 950 to 1250  $\text{cm}^{-1}$  can be very informative, where complicated strong absorption band profile of methylcellulose could be seen. This is mainly attributable to the C–O bonds' stretching vibrations in the cellulose and its ethers [53]. Another observation is that a reduction in the intensity of C–O bonds is seen in the doped samples. This confirms that there exists a strong interaction between the MC:Dext host blend polymer and incorporated salt. This apparent reduc-

tion of transmittance intensity and bands' shifting imply the process of complex formation between the salt cations and functional groups of the polymer blend matrix. Following the electrostatic interaction between salt cations and the functional groups of the host polymer, vibration of the polar groups can be reduced [11,39,54].

### 3.3. Morphological study

Acquiring images via scanning electron microscope (SEM) enables researchers to ensure the compatibility between different components of blend polymer electrolytes and determine phase separations, i.e., interfaces [41]. Furthermore, surface investigation provides benefits of understanding the structural and electrical properties changes under a number of processes. Previous studies have confirmed too much insight into changes over surfaces through the morphology views in polymers [8,55–57]. On the basis of crystallinity of polymer family, there is two extremes; crystalline and amorphous polymers. On one hand, the crystalline polymer features are compact assembly of stereo-regular chains; thereby, show high modulus and hardness but weak toughness. On the other hand, amorphous polymers are characterized by rubbery and glassy behavior [58]. In earlier work, the study the compatibility of salts with polar polymers was conducted via SEM [59–61]. Fig. 5(a–d) shows FESEM images for a number of MC:Dext systems doped with various weight percentages of  $\text{NH}_4\text{I}$  salt. The surface morphologies of the blend electrolyte samples revealed almost smooth surfaces and found no sign of protruded particles on them. This was, however, confirmed to be different in an earlier work, whereas more particles protruded out of the surface as more salts were added. Accordingly, polymer matrix capacity is limited to accommodate excess salt, which in turn led to salt recrystallization [62]. It is obvious that

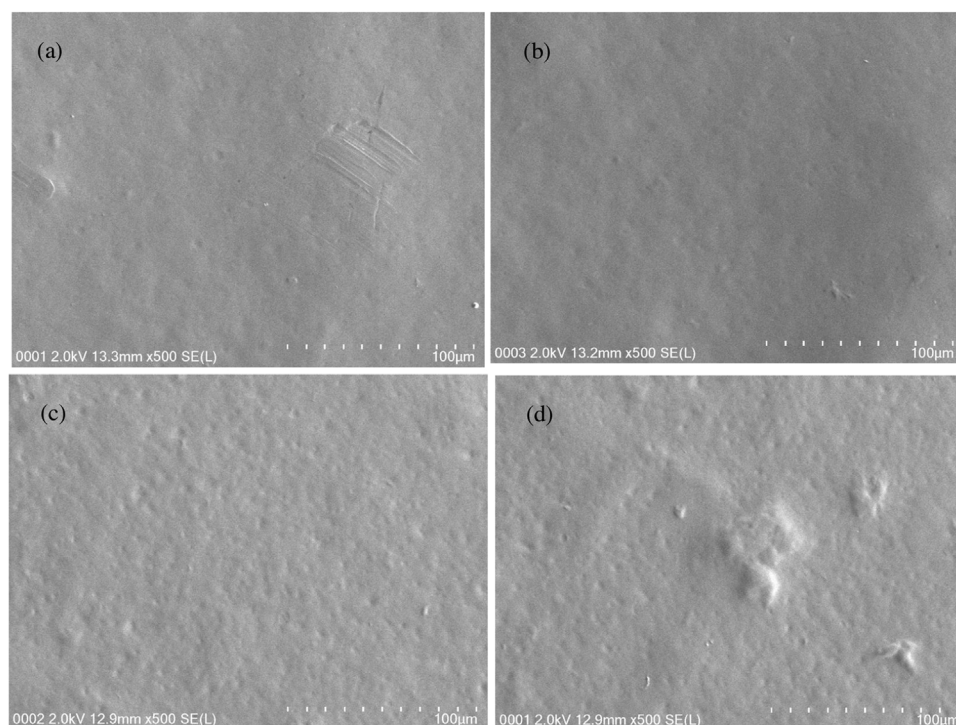


**Fig. 5 – FESEM images for (a) MCD1, (b) MCD2, (c) MCD3, and (e) MCD4 blend films.**

as re-crystallization proceeds, the amount of free ions lowers; in consequence, conductivity decreases [63].

There are various strategies that were applied in the attempt of overcoming several challenges. All these can be performed to gain deep understanding morphology thereby improves ion transport properties in polymer electrolytes. It is thought that in order to achieve high ion conductivity, the surface has to be smooth and having homogenous pores. In other words, it is correlated to the amorphous nature of the samples [33]. In fact, the complexation between the polymer blends and the incorporated  $\text{NH}_4\text{I}$  salt is evidenced by the smooth surface of the samples. In this work, the results show that there is a novelty of polymer blend fabrication as a new approach and an easy methodology to obtain relatively high DC conductivity. From the FTIR study, the complexation of the dopant salt and MC:Dext has been demonstrated. It is evidenced that the surface morphology of samples was found to be almost smooth without seen any noticeable protruded particles in the high rate incorporated  $\text{NH}_4\text{I}$  salt. From these findings, the synthesized polymer blending was defined by amorphous behavior even at high salt concentration.

### 3.4. Impedance study

In bulk materials, electrical charge displacements are carried out via two distinct physical phenomena; firstly, a polarization phenomenon, which occurs if the charge motion is strictly confined in a localized volume of the matter; secondly, collectively diffusion phenomenon, which is responsible for the electrical charges to be displaced over long distances in the materials and subsequently a dc conductivity ( $\sigma_{\text{dc}}$ ) is established [64]. It is self-evident that four different types of

polarization occur, once ac electric field is applied to a parallel plate capacitor separated by polymeric materials. These are electronic, atomic, dipolar and migrating charge polarization [65]. Firstly, ions are often regarded as impurities in the raw materials. Secondly, dipoles in atoms will occur with different electro negativities, which are bonded to each other on the backbone of polymeric materials [66].

From complex impedance spectroscopy (CIS) technique, one can take advantages of determination of relaxation frequency and distance between the opposite electrodes (low frequency spike) and bulk effects (high frequency semicircular region). The output of this technique comprises real ( $Z'$ ) and imaginary ( $Z''$ ) parts of impedance over a wide range of frequency. To the best of our knowledge, this technique has been successfully used for evaluation of the DC ionic conductivity and activation energy of ionic conductors [67]. The principle of CIS measurements is based on application of an alternating voltage on an electrochemical sample holder over a broad range of frequencies [68]. One of the outputs of electrical impedance spectroscopy (EIS) is a plot of the imaginary part of the impedance versus the real part. From this perturbation, the impedance plot is represented by the parallel combination of a resistor and a capacitor, and thereby  $Z_{\text{R-C}}$  has semicircular shape on the complex impedance plane as presented in Fig. 6(a,b) at high frequency regions. In this electrochemical cell perturbation, ion accumulation occurs at the electrode/electrolyte interfacial region, yielding the low frequency inclined data from electrode polarization. It is interesting to note that at the end of low frequency of the impedance plots, an incomplete semicircular shape is exhibited. This is qualitatively interpreted that the impedance of the capacitor is very large at that region. The majority of

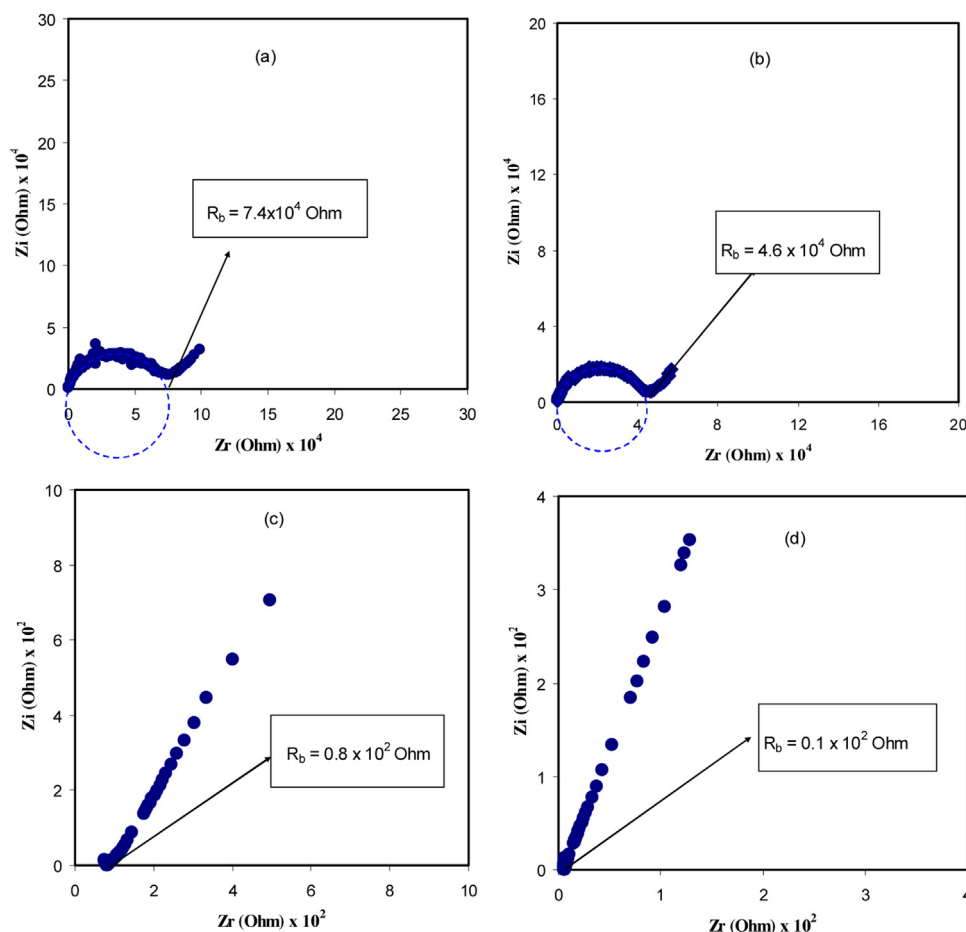


Fig. 6 – Impedance plots for (a) MCD1, (b) MCD2, (c) MCD3, and (d) MCD4 electrolyte films.

the current is, therefore, allowed to pass through the resistor, which dominates the behavior. However, the impedance of the capacitor is very small at very high frequency. It, thus, effectively shorts out the resistor, tending the total impedance toward zero [69]. It is shown in Fig. 6 that with an increase of salt concentration, there is a decrease in the bulk resistance (see the insets). In the analysis of the data point, the value of  $R_b$  is determined from the point, where the semicircle intersects the real axis ( $Z_r$ ). The sample conductivity has been determined based on the  $R_b$  value and the sample dimensions, using the following equation:

$$\sigma_{dc} = \left( \frac{1}{R_b} \right) \times \left( \frac{t}{A} \right) \quad (1)$$

where  $t$  and  $A$  are the thickness and surface area of the films, respectively.

The DC conductivity of systems is increasing with increasing salt concentrations (Table 1). This conductivity behavior of the electrolyte system is associated with increasing concentration of ions in the electrolytes coupled with high faster segmental motion of polymer blend chains in amorphous MC:Dex:NH<sub>4</sub>I electrolytes. The high DC conductivity of blend electrolytes is a guarantee for the application of the blend samples in EDLC devices.

Table 1 – DC conductivity for pure MC:Dex and blend electrolyte films at ambient temperature.

Sample designation	DC conductivity (S/cm)
MCD0	$6.5 \times 10^{-10}$
MCD1	$1.49 \times 10^{-7}$
MCD2	$2.41 \times 10^{-7}$
MCD3	$1.38 \times 10^{-4}$
MCD4	$1.12 \times 10^{-3}$

### 3.5. Energy storage EDLC study

#### 3.5.1. Transference number measurement (TNM)

TNM analysis is used to determine the main or dominant charge carrier species in the polymer electrolyte. The recorded current showed saturation at 0.20 V. The graph of polarization current versus time for the highest conducting electrolyte (MCD4) was obtained (see Fig. 7). The large value of the initial current is assigned to the participation of both ion and electron conduction at the initial stage. Fig. 7 revealed that the current has decayed drastically prior to reach the steady state. In the steady state, the cell is polarized to large extent and the remaining current flow is due to electron. This is due to the ionic blocking effect by stainless steel electrodes, where electron is a unique entity pass through [70]. The cell was sub-

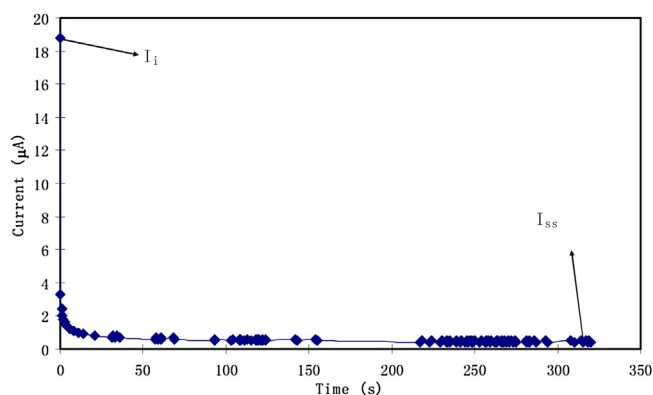


**Fig. 7 – Polarization current versus time for the highest conducting (MCD4) electrolyte film.**

jected to 0.20 V at room temperature.  $t_i$  was identified using the following equation [71]:

$$t_i = \frac{I_i - I_{ss}}{I_i} \quad (2)$$

$$t_i = 1 - t_e \quad (3)$$

where  $I_{ss}$  and  $I_i$  are the steady state and initial current, respectively.

The values of  $t_i$  and  $t_e$  are obtained from both Eqs. (2 and 3) and the values of  $I_i$  and  $I_{ss}$  were extracted and found to be 18.8  $\mu\text{A}$  and 0.4  $\mu\text{A}$ , respectively. The  $t_i$  value was 0.98 and found to be of vital interest because of very closeness to its ideal value of unity. As a consequence, in MC:Dext:NH<sub>4</sub>I system, ions are found to be responsible the migration process of the charge carriers. This finding is comparable to the system of Potato starch (PS)-methyl cellulose (MC) blend solid biopolymer electrolytes mixed with ammonium nitrate (NH<sub>4</sub>NO<sub>3</sub>) and glycerol as plasticizer (PS-MC-NH<sub>4</sub>NO<sub>3</sub>-glycerol-based electrolytes), which is documented by Hamsan et al. [72]. In comparison, the ionic transference number obtained in the current work is quite similar to earlier studies. Polu et al. [73,74] have studied the ionic transference numbers of PVA-Mg(CH<sub>3</sub>COO)<sub>2</sub> and PVA-Mg(NO<sub>3</sub>)<sub>2</sub> and found to be 0.96 and 0.98, respectively. Wang et al. [75] have examined that the ionic transference numbers of PVA-LiTFSI-EMITFSI is 0.995.

### 3.5.2. Electrochemical stability study

In this section, the LSV method is used to determine the electrochemical stability of the highest conducting MC:Dext:NH<sub>4</sub>I system. Fig. 8 shows the LSV plot of the sample. The voltage was swept over a potential range of 0 V to 2.5 V at a scan rate of 100 mV s<sup>-1</sup>, a large current is observed at certain potentials. This was cut-off current resulted from the decomposition of electrolyte at the inert electrode [76]. In MC:Dext:NH<sub>4</sub>I system, it is found to be stable up to 1.27 V, which is appropriate at the sufficient range for proton based energy device applications. Pratap et al. [77] have studied the standard electrochemical window of proton batteries, which was recorded to be ~1 V. In the present work, the recorded breakdown voltage of methylcellulose-dextran blend polymer electrolyte was found to be relatively high enough in order to be used safely in the

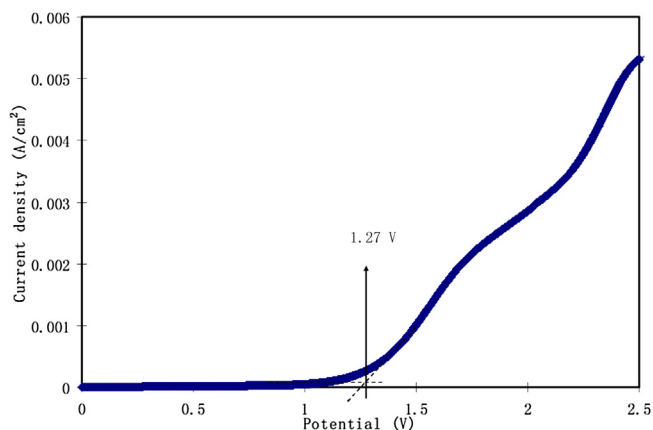


**Fig. 8 – Linear sweep voltammetry (LSV) plot for the highest conducting (MCD4) blend electrolyte.**

application of any protic electrolyte devices. Therefore, based on this finding, it can be concluded that the highest conducting MC:Dext:NH<sub>4</sub>I SPE film is electrochemically durable to be applied in electrochemical devices, for instance, in proton battery application. An incredible interest in this study is comparability with the results obtained in ammonium salt based polymer electrolytes. Kadir et al. [33] have examined a plasticized system of methyl cellulose (MC) incorporated with NH<sub>4</sub>Br, in which the electrochemical stability was obtained up to 1.53 V. In another study conducted by Woo et al. [78], poly ( $\epsilon$ -caprolactone) (PCL)-based polymer electrolytes was found to electrochemically durable up to 1.4 V.

In the present study, the decomposition voltage of the polymer electrolyte was around 1.27 V. In a comparison, it is well-reported that the decomposition voltage of blend biopolymer electrolyte containing starch/chitosan incorporated with ammonium iodide and plasticized with glycerol has the decomposition voltage of 1.90 V, which is larger than the outcome achieved in our work [79]. However, MC:Dext:NH<sub>4</sub>I system is verified to be more compatible for application in EDLC, based on the EDLC characterizations performed as being explained in the next sections.

### 3.5.3. Cyclic voltammetry (CV) study

The nature of charge storage at the electrode-electrolyte interfaces in EDLCs can be deeply conducted through the cyclic voltammetric. The analysis of the nature of charge storage at the interfacial region in the anodic and cathodic regions can be obtained from CV of the EDLC cells [2]. Fig. 9 exhibits the CV of the assembled cell at room temperature. Firstly, there is no peak in the polarization curve, indicating that no redox reaction takes place in the potential range of 0–0.90 V. This phenomenon strongly proves the existence of electrical double layer capacitors [80]. The charge storage mechanism in EDLC is based on the ion accumulation at the electrode-electrolyte interfaces under an electric potential perturbation [81]. The figure shows a nearly rectangular shape of CV, which shows a capacitor behavior. Compared to those reported in the literature, which are quite close to leaf-like shape [78,81]. An ideal EDLC has a perfect rectangular shape CV. The high scan rate causes a discrepancy of



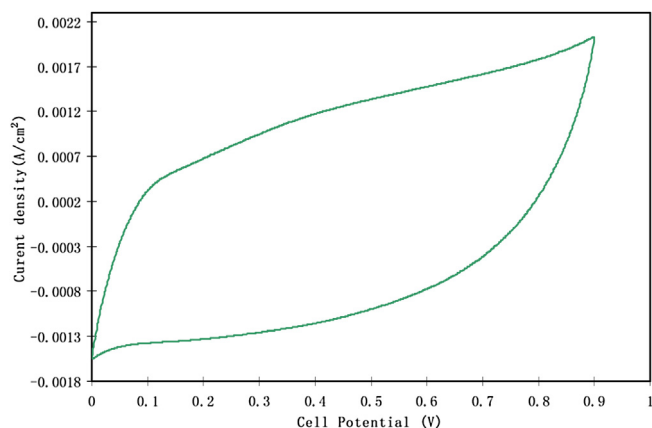


**Fig. 9 – Cyclic voltammetry (CV) plot of the fabricated electrical double layer capacitor (EDLC) for MCD4 film in the potential range of 0 V–0.90 V.**

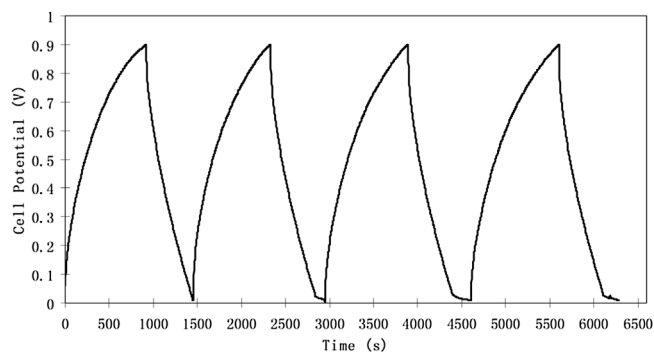
the cyclic voltammogram shape from a perfect rectangular shape, which might be ascribed to both carbon porosity and the internal resistance, thereby creating a current dependence of voltage [82]. The mechanism of charge storage in EDLC device is still a subject of debate. Dealing with the mechanism of energy storage, microporous materials can be crucial for both fundamental and industrial aspects. The great advance in designing super-capacitors with a relatively high performance has enabled researchers to develop such technology for industrial applications in very close future. It is also considered as a breakthrough to some extent in the field of super-capacitor fabrication. Moreover, researchers have been encouraged to verify that the mechanism of charge storing—in terms of experimentation and theory—is necessary [83]. Eftekhari [84] has, however, shown a review, where the energy storage mechanism is based on housing of ions inside microporous and mesopores somewhat than the formation of a double layer capacitor. Consequently, this mechanism is dissimilar to some level from the classical model, in which the ions aid the charge separation and storage in energy storage devices. On the other hand, the classical models are based on the inner layer, which is formed due to the electrostatic forces; thereby the charged species are accumulated on the surface of the electrode without any real chemical interaction. Therefore, the double layer charging on the electrode surface should be ideally polarizable [85].

#### 3.5.4. Charge-discharge characterization

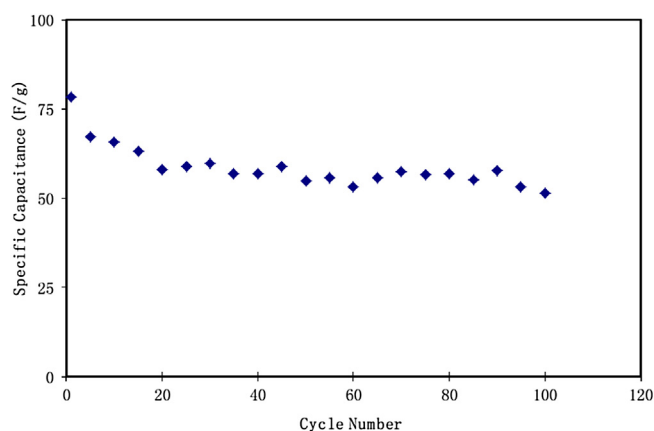
Fig. 10 shows galvanostatic charge–discharge characteristics of the fabricated EDLC. The gradient of the discharge parts are almost linear, suggesting the presence of charge double-layer and capacitive characteristics [86]. The specific capacitance ( $C_{sp}$ ) of the EDLC,

$$C_{sp} = \frac{i}{gm} \quad (4)$$

where,  $i$  is the operating current,  $g$  is the gradient of discharge curve and  $m$  is the active material's mass. From the gradient of discharge curve, the value of  $C_{sp}$  is calculated, using Eq. (4).



**Fig. 10 – Charge-discharge profiles for the fabricated EDLC at 0.5 mA cm<sup>-2</sup>.**

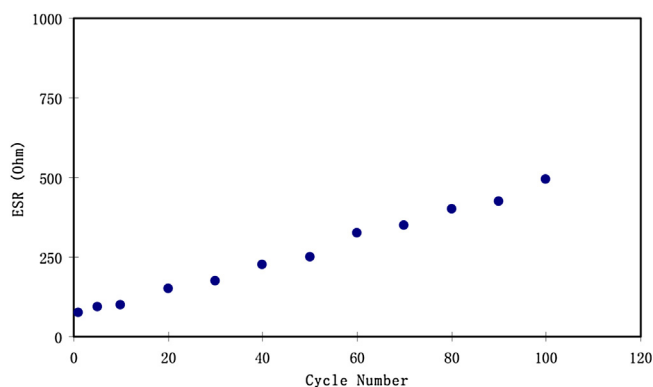


**Fig. 11 – Specific capacitance of the fabricated EDLC for 100 cycles.**

Fig. 11 shows the plot of  $C_{sp}$  against cycle number for the fabricated EDLC. The value of  $C_{sp}$  acquired for the 1st cycle was found to be 79 F g<sup>-1</sup>, whereas it dropped to 55 F g<sup>-1</sup> at the 20th cycle. The value of  $C_{sp}$  has remained almost constant over the cycles beyond the 20th cycle till it completed 100 cycles. The relatively high in the capacitance value for the first cycle in EDLCs/supercapacitors is ascribed to the fast build-up of the double layers as well as the contribution of both ion and electron at the initial stage. After the first cycle, the initial decrease in the  $C_{sp}$  values toward the 20th cycle is noticed in Fig. 11, which is due to the current decayed before reaching the steady state. In earlier reports large reduction of  $C_{sp}$  was noticed with increasing the number of cycles. It is believed the reduction of these electrochemical properties of EDLC belongs to the formation of ion aggregation. Indeed, the mobile ions prefer to be paired up or aggregated beyond the rapid charge and discharge processes. These ion pairs can block the ionic transportation in the polymer electrolyte and consequently influence ion adsorption into the pores of carbon, which decreases the creation of ion adsorption at the electrode–electrolyte interface region. Therefore, the specific capacitance, energy density and power density of EDLC decrease with increasing the cycle number as a result, the electrochemical properties, such as the specific capacitance, energy density and power density of EDLC decrease as the number of cycle increases [87]. The obtained value of  $C_{sp}$  in the present work is greater than that

**Table 2 – Capacitance of EDLCs using different solid polymer electrolytes.**

Polymer electrolytes	Electrode material	Cs(F g <sup>-1</sup> )	References
PEO-Mg(Tf)2 + EMITf	MWCNTs-AB-PVdF-HFP	2.6–3.0	[2]
Nafion/PTFE composite polymer	carbon	16	[88]
Chitosan-κ-carrageenan-NH <sub>4</sub> NO <sub>3</sub>	Activated carbon	18.5	[89]
Chitosan-PVA-NH <sub>4</sub> NO <sub>3</sub> -EC	Activated carbon	27.1	[82]
MC-PS-NH <sub>4</sub> NO <sub>3</sub> -glycerol	Activated carbon	31	[72]
MC-NH <sub>4</sub> NO <sub>3</sub> -PEG	PEG coated with activated carbon	38	[90]
Polyvinylalcohol-polystyrene sulphonic	carbon	40	[91]
Cellulose acetate-LiClO <sub>4</sub>	p/p polypyrrole	90	[92]
Methylcellulose-dextran-NH <sub>4</sub> I	Activated carbon	79	Present work

**Fig. 12 – The pattern of the equivalent series resistance of the EDLC for 100 cycles.**

reported in the literature. The value of  $C_{sp}$  of the fabricated EDLC is compared to other reports using various polymer electrolytes as listed in Table 2.

From Fig. 10, one can see a potential drop prior starting of every discharge process. This is associated to the presence of an internal resistance called equivalent series resistance ( $R_{es}$ ). The EDLC parameters, such as  $R_{es}$ , energy density ( $E$ ) and power density ( $P$ ), can be calculated using the following equations [93]:

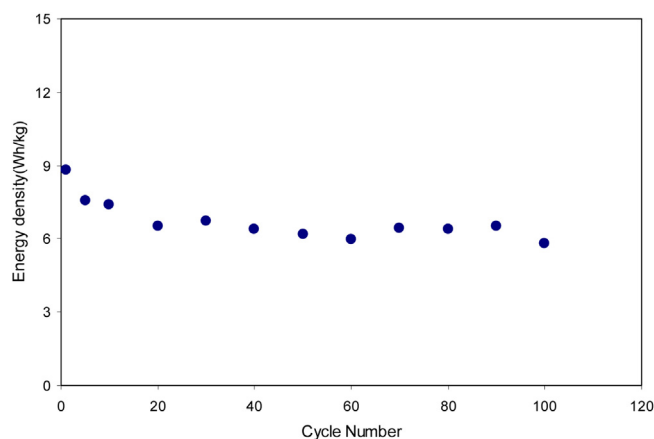
$$R_{es} = \frac{V_{drop}}{i} \quad (5)$$

$$E = \frac{C_s V}{2} \quad (6)$$

$$P = \frac{V^2}{4mR_{es}} \quad (7)$$

where  $V_{drop}$  stands for voltage drop before discharging process and  $V$  is the voltage applied.

From Fig. 12, the value of  $R_{es}$  was found to be varied from 75 to 493  $\Omega$ . The logical explanation of the existence of  $R_{es}$  in the EDLC is mainly due to three resistances; current collector, the bulk of the electrolyte as well as the interfacial region between electrolyte and electrodes [94]. Kumar and Bhat [91] have examined such increase in voltage drop throughout the charge-discharge cycle, which led to an increase in ESR as a result of the degradation of the solid polymer electrolytes in the EDLC. In the present work, the ESR of the EDLC is quite low if it compared to that (1300  $\Omega$ ) documented for ionic liquid

**Fig. 13 – Energy density of the fabricated EDLC for 100 cycles.**

incorporated with Poly(ethylene oxide) (PEO) based polymer electrolyte [2].

The value of  $E_d$  calculated from Eq. (6) can be seen in Fig. 13. From the figure, the value of  $E_d$  at the 1st cycle is 8.81 Wh/kg. The  $E_d$  value then decreases for few cycles and then nearly constant at 6.3 Wh/kg in average from the 20th cycle to the 100th cycle. Hence, it can be assumed that the ion migration possesses nearly similar energy barrier in this cycle range [21]. In fact, this decreasing in  $E_d$  value throughout the cycle number is mainly owing to an increase in the internal resistance, leading to the increment of energy loss during the process of charging and discharging cycle [82,95].

The achieved energy density for the EDLC cell is large enough compared to that reported (0.3 Wh/kg) for ionic liquid incorporated with PEO based polymer electrolyte [2]. The energy density obtained in the current work is of the large interest compared to the energy density values of 2.2 Wh/kg which obtained for EDLC of the system of methylcellulose (MC)-starch-NH<sub>4</sub>NO<sub>3</sub> [72]. Moreover, the energy density of the present work (6.3 Wh/kg) is of great interest compared to the values reported (1.4 Wh/kg and 0.86 Wh·kg<sup>-1</sup>) in our previous works for Chitosan:Dextran incorporated with NH<sub>4</sub>F and LiClO<sub>4</sub> salts, respectively [96,97]. While, it is lower to that obtained (8.63 Wh·kg<sup>-1</sup>) for biopolymer blend electrolytes inserted with NH<sub>4</sub>SCN [98]. These results indicate that the type of salts and designing of polymer blends based on natural resources has great effects on the performance of EDLC devices.

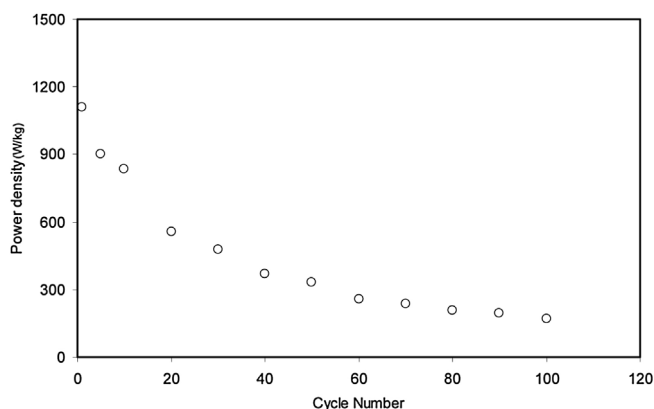


**Fig. 14 – Power density of the fabricated EDLC for 100 cycles.**

The calculated value of power density ( $P_d$ ) from Eq. (7) is seen in Fig. 14. Upon charge-discharging over 100 cycles, the  $P_d$  of the EDLC shows a drastic drop from 1111.1–170.0 W/kg. The outcome of the current study is comparable with that reported by Shukur et al. [93]. The value of  $P_d$  is lowered as the cycle number increased. This decline trend harmonized with the raising trend of  $R_{es}$  in Fig. 12. The increment of internal resistance is caused by the depletions of the electrolyte and aggregation of ions regarding a fast charge and discharge mechanism; therefore, it provides lower power density at large cycle number [99]. The decrease of specific power density, energy density, and capacitance is owing to the electrolyte depletion. Ion agglomeration after the fast charged and discharged processes will block the ionic movements toward the surface of the electrodes which cause a decrease of ion adsorption at the electrode–electrolyte interface [87].

#### 4. Conclusions

In conclusion, polymer blend electrolyte films comprising methylcellulose:dextran (MC:Dex) blend doped with various amounts of ammonium iodide ( $NH_4I$ ) are crucial for EDLC application. The shifting in the band positions and relative decrease in their intensities observed in the FTIR studies corroborate the complexation between the MC:Dex and  $NH_4I$ . The XRD studies reveal the enhancement in the amorphous nature of electrolyte systems with increasing salt concentration. The DC conductivity is found to be increasing with increasing the salt concentration and maximum conductivity is found to be  $1.12 \times 10^{-3}$  S/cm for composition with 40 wt% of  $NH_4I$ . The electrolyte system is predominantly ionic in nature. From LSV analysis, MC:Dex: $NH_4I$  electrolyte is found to be electrochemically stable up to 1.27 V. The DC conductivity value, TNM and LSV results reveal the availability of the samples for electrical double layer capacitor (EDLC) application. The existence of charges double-layer in the fabricated EDLC is proven from cyclic voltammetry (CV). The fabricated EDLC offers an initial specific capacitance as 79 F/g, energy density as 8.81 Wh/kg and power density as 1111.0 W/kg at a current density of 0.2 mA/cm<sup>2</sup>. Fading is observed in the EDLC performance in prolonged cyclic tests. The results shown in the present work indicate that the above electrolyte system comprising poly-

mers obtained from natural resources have potential to be used in EDLC devices.

#### Conflicts of interest

The authors declare no conflicts of interest.

#### Acknowledgement

The authors gratefully acknowledge the financial support for this study from Ministry of Higher Education and Scientific Research-Kurdish National Research Council (KNRC), Kurdistan Regional Government/Iraq. The financial support from the University of Sulaimani and Komar Research Center (KRC), Komar University of Science and Technology are greatly appreciated.

#### REFERENCES

- [1] Kumar Yogesh, Pandey GP, Hashmi SA. Gel polymer electrolyte based electrical double layer capacitors: comparative study with multiwalled carbon nanotubes and activated carbon electrodes. *J. Phys. Chem. C* 2012;116:26118–27.
- [2] Pandey GP, Kumar Yogesh, Hashmi SA. Ionic liquid incorporated PEO based polymer electrolyte for electrical double layer capacitors: a comparative study with lithium and magnesium systems. *Solid State Ion* 2011;190:93–8.
- [3] Alexandre Sandra A, Silva Glauro G, Santamaría Ricardo, Trigueiro João Paulo C, Lavall Rodrigo L. A highly adhesive PII/IL gel polymer electrolyte for use in flexible solid state supercapacitors. *Electrochim Acta* 2019;299:789–99.
- [4] Aziz Shujahadeen B, Abidin ZHZ, Arof Abdul Kariem. Effect of silver nanoparticles on the DC conductivity in chitosan–silver triflate polymer electrolyte. *Physica B* 2010;405:4429–33.
- [5] Nyuk CM, Isa MIN. Solid biopolymer electrolytes based on carboxymethyl cellulose for use in coin cell proton batteries. *Journal of Sustainability Science and Management* 2018;2017:42–8.
- [6] Chong, Yoke Mee. Development of biodegradable solid polymer electrolytes incorporating different nanoparticles for electric double layer capacitor PhD thesis. University of Malaya; 2017.
- [7] Salleh N, Aziz SB, Aspanut Z, Kadir M. Electrical impedance and conduction mechanism analysis of biopolymer electrolytes based on methyl cellulose doped with ammonium iodide. *Ionics* 2016;22:2157–67.
- [8] Hamsan MH, Aziz Shujahadeen B, Shukur MF, Kadir MFZ. Protonic cell performance employing electrolytes based on plasticized methylcellulose–potato starch- $NH_4NO_3$ . *Ionics* 2019;25:559–72.
- [9] Stepniak I, Galinski M, Nowacki K, Wysokowski M, Jakubowska P, Bazhenov V, et al. A novel chitosan/sponge chitin origin material as a membrane for supercapacitors–preparation and characterization. *RSC Adv* 2016;6(5):4007–13.
- [10] Aziz SB.  $Li^+$  ion conduction mechanism in poly ( $\epsilon$ -caprolactone)-based polymer electrolyte. *Iran Polym J* 2013;22:877, <http://dx.doi.org/10.1007/s13726-013-0186-7>.
- [11] Aziz Shujahadeen B, Abidin Zul Hazrin Z. Electrical conduction mechanism in solid polymer electrolytes: new concepts to arrhenius equation. *J Soft Matter* 2013,

- <http://dx.doi.org/10.1155/2013/323868>. Article ID 323868, 8 pages.
- [12] Sudhakar Y, Selvakumar M, Bhat DK. Preparation and characterization of phosphoric acid-doped hydroxyethyl cellulose electrolyte for use in supercapacitor. *Mater Renew Sustain Energy* 2015;4(3):1–9.
  - [13] Hassan MF, Azimi NSN, Kamarudin KH, Sheng CK. Solid polymer electrolytes based on starch-magnesium sulphate: study on morphology and electrical conductivity. *ASM Sci. J. Special Issue* 2018;1:17–28.
  - [14] Du BW, Hu SY, Singh R, Tsai TT, Lin CC, Ko FU. Eco-friendly and biodegradable biopolymer Chitosan/Y2O3 composite materials in flexible organic thin-film transistors. *Materials* 2017;10:1026.
  - [15] Moniha V, Alagar M, Selvasekarapandian S, Sundaresan B, Hemalatha R, Boopathi G. Synthesis and characterization of bio-polymer electrolyte based on iota-carrageenan with ammonium thiocyanate and its applications. *J Solid State Electrochem* 2018;22:3209–23.
  - [16] Hamsan MH, Shukur MF, Aziz SB, Kadir MFZ. Dextran from *Leuconostoc mesenteroides*-doped ammonium salt-based green polymer electrolyte. *Bull Mater Sci* 2019;42:57, <http://dx.doi.org/10.1007/s12034-019-1740-5>.
  - [17] Mantravadi R, Chinnam PR, Dikin DA, Wunder SL. High conductivity, high strength solid electrolytes formed by in situ encapsulation of ionic liquids in nanofibrillar methyl cellulose networks. *ACS Appl Mater Interf* 2016;21:13426–36.
  - [18] Chai MN, Isa MIN. The oleic acid composition effect on the carboxymethyl cellulose based biopolymer electrolyte. *J. Cryst. Proc. Technol* 2013;3:1–4.
  - [19] Rengui W, Lihui C, Shan L, Hui Z, Hui W, Kai L, et al. Preparation and characterization of antibacterial Cellulose/Chitosan nanofiltration membranes. *Polymers* 2017;9:116.
  - [20] Taghizadeh MT, Seifi-Aghjekohal P. Sonocatalytic degradation of 2-hydroxyethyl cellulose in the presence of some nanoparticles. *Ultrason Sonochem* 2015;26:265–72.
  - [21] Shukur MF. Characterization of ion conducting solid biopolymer electrolytes based on starch-chitosan blend and application in electrochemical devices. Malaysia: Dissertation, University of Malaya; 2015.
  - [22] Shuhaimi NEA, Teo LP, Majid SR, Arof AK. Transport studies of NH4NO3 doped methyl cellulose electrolyte. *Synth Met* 2010;160:1040–4.
  - [23] Pinotti A, Garci MA, Martino MN, Zaritzky NE. Study on microstructure and physical properties of composite films based on chitosan and methylcellulose. *Food Hydrocoll* 2007;21:66–72.
  - [24] Hamsan MH, Shukur MF, Kadir MFZ. The effect of NH4NO3 towards the conductivity enhancement and electrical behavior in methyl cellulose-starch blend based ionic conductors. *Ionics* 2017;23:1137–54.
  - [25] Kadir MFZ, Hamsan MH. Green electrolytes based on dextran-chitosan blend and the effect of NH4SCN as proton provider on the electrical response studies. *Ionics* 2018;24(8):2379–98.
  - [26] Abdullah Ranjdar M, Aziz Shujahadeen B, Mamand Soran M, Hassan Aso Q, Hussein Sarkawt A, Kadir MFZ. Reducing the crystallite size of spherulites in PEO-Based polymer nanocomposites mediated by carbon nanodots and Ag nanoparticles. *Nanomaterials* 2019;9(6):874, <http://dx.doi.org/10.3390/nano9060874>.
  - [27] Wang Longlu, Zhanga Qingfeng, Zhu Jingyi, Duan Xidong, Xu Zhi, Liu Yutang, et al. Nature of extra capacity in MoS2 electrodes: molybdenum atoms accommodate with lithium. *Energy Storage Mater* 2019;16:37–45.
  - [28] Zhang Qingfeng, Wang Longlu, Wang Jue, Yu Xinzh, Ge Junmin, Zhang Hang, et al. Semimetallic vanadium molybdenum sulfide for high-performance battery electrodes. *J Mater Chem A* 2018;6:9411–9.
  - [29] Iro Zaharaddeen S, Subramani C, Dash SS. A Brief Review on Electrode Materials for Supercapacitor. *Int J Electrochem Sci* 2016;11:10628–43.
  - [30] Inagaki M, Konno H, Tanaike O. Carbon materials for electrochemical capacitors. *J Power Sources* 2010;195(24):7880–903.
  - [31] Zhang D, Zhang X, Chen Y, Yu P, Wang C, Ma Y. Enhanced capacitance and rate capability of graphene/polypyrrole composite as electrode material for supercapacitors. *J Power Sources* 2011;196(14):5990–6.
  - [32] Pell WG, Conway BE. Peculiarities and requirements of asymmetric capacitor devices based on combination of capacitor and battery-type electrodes. *J Power Sources* 2004;136(2):334–45.
  - [33] Kadir MFZ, Salleh NS, Hamsan MH, Aspanut Z, Majid NA, Shukur MF. Biopolymeric electrolyte based on glycerolized methyl cellulose with NH4Br as proton source and potential application in EDLC. *Ionics* 2017;24:1651–62.
  - [34] Kamarudin KH, Hassan M, Isa MIN. Lightweight and flexible solid-state EDLC based on optimized CMC-NH4NO3 solid bio-polymer electrolyte. *ASM Sci J* 2018;1:29–36.
  - [35] Wang H, Lin J, Shen ZX. Polyaniline (PANI) based electrode materials for energy storage and conversion. *J Sci Adv Mater Devices* 2016;1:225–55.
  - [36] Yang Hezhen, Liu Ying, Kong Lingbin, Kang Long, Ran Fen. Biopolymer-based carboxylated chitosan hydrogel film crosslinked by HCl as gel polymer electrolyte for all-solid-state supercapacitors. *J Power Sources* 2019;426:47–54.
  - [37] Liu P, Xiangmei W, Zhong L. Miscibility study of chitosan and methylcellulose blends. *Adv Mater Res* 2013;750–752: 802–5.
  - [38] Nik Aziz NA, Idris NK, Isa MIN. Solid polymer electrolytes based on methylcellulose: FT-IR and ionic conductivity studies. *Int J Polym Anal Charact* 2010;15:319–27.
  - [39] Aziz Shujahadeen, Rasheed Mariwan, Ahmed Hameed. Synthesis of polymer nanocomposites based on [Methyl Cellulose](1– x):(CuS) x (0.02 m ≤ x ≤ 0.08 m) with desired optical band gaps. *Polymers* 2017;9(6):194, <http://dx.doi.org/10.3390/polym9060194>.
  - [40] Aziz Shujahadeen B, Abdullah Ranjdar M. Crystalline and amorphous phase identification from the tanδ relaxation peaks and impedance plots in polymer blend electrolytes based on [CS: AgNt] x: PEO (x-1)(10 ≤ x ≤ 50). *Electrochim Acta* 2018;285:30–46.
  - [41] Vanitha D, Bahadur SA, Nallamuthu Sh, Athimoolam A, Manikandan. Electrical impedance studies on sodium ion conducting composite blend polymer electrolyte. *J Inorg Organomet Polym Mater* 2017;27:257, <http://dx.doi.org/10.1007/s10904-016-0468-6>.
  - [42] Aziz Shujahadeen B, Rasheed Mariwan A, Hussein Ahang M, Ahmed Hameed M. Fabrication of polymer blend composites based on [PVA-PVP](1– x):(Ag2S) x (0.01 ≤ x ≤ 0.03) with small optical band gaps: structural and optical properties. *Mater Sci Semicond Process* 2017;71:197–203.
  - [43] Aziz SB. Role of dielectric constant on ion transport: reformulated Arrhenius equation. *Adv Mater Sci Eng*, Volume 2016, <http://dx.doi.org/10.1155/2016/2527013>. Article ID 2527013, 11 pages.
  - [44] Aziz SB, Abidin ZHZ. Ion-transport study in nanocomposite solid polymer electrolytes based on chitosan: electrical and dielectric analysis. *J Appl Polym Sci* 2015;132: 41774.
  - [45] Hodge RM, Edward GH, Simon GP. Water absorption and states of water in semicrystalline poly(vinyl alcohol) films. *Polym J* 1996;37:1371–6.



- [46] Turhan KN, Ahbaz FS, Guner A. A spectrophotometric study of hydrogen bonding in methylcellulose-based edible films plasticized by polyethylene glycol. *J Food Sci* 2001;66:59–62.
- [47] Aziz NAN, Idris NK, Isa MIN. Solid polymer electrolytes based on methylcellulose: FT-IR and ionic conductivity studies. *Int J Polym Anal Charact* 2010;15:319–27.
- [48] Vettori Mary Helen Palmuti Braga, Franchetti Sandra Mara Martins, Contiero Jonas. Structural characterization of a new dextran with a low degree of branching produced by *Leuconostoc mesenteroides* FT045B dextranase. *Carbohydr Polym* 2012;88:1440–4.
- [49] Dumitrascu M, Meltzer V, Sima E, Virgolici M, Albu MG, Fica A, et al. Characterization of electron beam irradiated collagen-polyvinylpyrrolidone (PVP) and collagen-dextran (DEX) blends. *Dig J Nanomater Biostruct* 2011;6(October-December (4)):1793–803.
- [50] Zhu YS, Xiao SY, Li MX, Chang Z, Wang FX, Gao J, et al. Natural macromolecule based carboxymethyl cellulose as a gel polymer electrolyte with adjustable porosity for lithium ion batteries. *J Power Sources* 2015;288:368–75.
- [51] Tunç S, Duman O, Polat TG. Effects of montmorillonite on properties of methyl cellulose/carvacrol based active antimicrobial nanocomposites. *Carbohydr Polym* 2016;150:259–68.
- [52] Devi CU, Sharma AK, Rao VVRN. Electrical and optical properties of pure and silver nitrate-doped polyvinyl alcohol films. *Mater Lett* 2002;56:167–74.
- [53] Buslov DK, Sushko NI, Tretinnikov ON. Study of thermal gelation of methylcellulose in water using FTIR-ATR spectroscopy. *J Appl Spectrosc* 2008;75:514–8.
- [54] Wei D, Sun W, Qian W, Ye Y, Ma X. The synthesis of chitosan-based silver nanoparticles and their antibacterial activity. *Carbohydr Res* 2009;344:2375–82.
- [55] Aziz SB, Abidin ZHZ, Kadir MFZ. Innovative method to avoid the reduction of silver ions to silver nanoparticles in silver ion conducting based polymer electrolytes. *Phys Scr* 2015;90, 035808 (9pp).
- [56] Aziz Shujahadeen B, Abidin Zul Hazrin Z. Electrical and morphological analysis of chitosan: AgTf solid electrolyte. *Mater Chem Phys* 2014;144:280–6.
- [57] Aziz Shujahadeen, Abdullah Ranjdar, Rasheed Mariwan, Ahmed Hameed. Role of ion dissociation on DC conductivity and silver nanoparticle formation in PVA: AgNt based polymer electrolytes: deep insights to ion transport mechanism. *Polymers* 2017;9(8):338, <http://dx.doi.org/10.3390/polym9080338>.
- [58] Hana Charles C, Shia Weichao, Jin Jing. Morphology and crystallization of Crystalline/Amorphous polymer blends. *Encyclopedia Polym Compos* 2013:1–19, [http://dx.doi.org/10.1007/978-3-642-37179-0\\_25-1](http://dx.doi.org/10.1007/978-3-642-37179-0_25-1).
- [59] Aziz SB, Abdullah RM, Kadir MFZ, Ahmed HM. Non suitability of silver ion conducting polymer electrolytes based on chitosan mediated by barium titanate (BaTiO<sub>3</sub>) for electrochemical device applications. *Electrochim Acta* 2019;296:494–507, <http://dx.doi.org/10.1016/j.electacta.2018.11.081>.
- [60] Aziz SB. The mixed contribution of ionic and electronic carriers to conductivity in chitosan based solid electrolytes mediated by CuNt salt. *J Inorg Organomet Polym Mater* 2018;28:1942, <http://dx.doi.org/10.1007/s10904-018-0862-3>.
- [61] Aziz SB, Brza MA, Mohamed Pshko A, Kadir MFZ, Hamsan MH, Abdulwahid Rebar T, et al. Increase of metallic silver nanoparticles in Chitosan: AgNt based polymer electrolytes incorporated with alumina filler. *Results Phys* 2019;13:102326.
- [62] Aziz SB. Morphological and optical characteristics of chitosan (1– x): cuox (4 ≤ x ≤ 12) based polymer nano-composites: optical dielectric loss as an alternative method for tauc's model. *Nanomaterials* 2017;7(12):444, <http://dx.doi.org/10.3390/nano7120444>.
- [63] Shukur MF, Kadir MFZ. Hydrogen ion conducting starch-chitosan blend based electrolyte for application in electrochemical devices. *Electrochim Acta* 2015;158:152–65, <http://dx.doi.org/10.1016/j.electacta.2015.01.167>.
- [64] Shujahadeen BA, Woo Thompson J, Kadir MFZ, Ahmed Hameed M. A conceptual review on polymer electrolytes and ion transport models. *J Sci Adv Mater Devices* 2018;3:1–17.
- [65] Nicolau A, Nucci AM, Martini EMA, Samios D. Electrical impedance spectroscopy of epoxy systems II: molar fraction variation, resistivity, capacitance and relaxation processes of 1,4-butanediol diglycidyl ether/succinic anhydride and triethylamine as initiator. *Eur Polym J* 2007;43:2708–17.
- [66] Nahm SH. Use of dielectric spectroscopy for real-time in-situ reaction monitoring. *JCT Res* 2006;3:257e265.
- [67] Mahato DK, Dutta A, Sinha TP. Impedance spectroscopy analysis of double perovskite Ho<sub>2</sub>NiTiO<sub>6</sub>. *J Mater Sci* 2010;45:6757–62.
- [68] Fortunato R, Branco LC, Afonso CAM, Benavente J, Crespo JG. Electrical impedance spectroscopy characterisation of supported ionic liquid membranes. *J Membr Sci* 2006;270:42–9.
- [69] Huggins RA. Simple method to determine electronic conductivity in mixed and ionic components of the conductors. *Ionics* 2002;8:300–13.
- [70] Rani MSA, Ahmad A, Mohamed NS. Influence of nano-sized fumed silica on physicochemical and electrochemical properties of cellulose derivatives-ionic liquid biopolymer electrolytes. *Ionics* 2017;24:807–14.
- [71] Tripathi Mukta, Tripathi SK. Electrical studies on ionic liquid-based gel polymer electrolyte for its application in EDLCs. *Ionics* 2017;23:2735, <http://dx.doi.org/10.1007/s11581-017-2051-8>.
- [72] Hamsan MH, Shukur MF, Kadir MFZ. NH<sub>4</sub>NO<sub>3</sub> as charge carrier contributor in glycerolized potato starch-methyl cellulose blend-based polymer electrolyte and the application in electrochemical double-layer capacitor. *Ionics* 2017;23:3429–53.
- [73] Polu AR, Kumar R. Ionic conductivity and discharge characteristic studies of PVA-Mg(CH<sub>3</sub>COO)<sub>2</sub> solid polymer electrolytes. *Int J Polym Mater Polym Biomater* 2013;62:76–80.
- [74] Polu AR, Kumar R. Preparation and characterization of pva based solid polymer electrolytes for electrochemical cell applications. *Chin J Polym Sci* 2013;31:641–8.
- [75] Wang Jingwei, Zhao Zejia, Song Shenhua, Ma Qing, Liu Renchen. High performance poly(vinyl alcohol)-Based Li-Ion conducting gel polymer electrolyte films for electric double-layer capacitors. *Polymers* 2018;10:1179.
- [76] Tian Khoo L, Ataollahi N, Hassan NH, Ahmad A. Studies of porous solid polymeric electrolytes based on poly (vinylidene fluoride) and poly (methyl methacrylate) grafted natural rubber for applications in electrochemical devices. *J Solid State Electrochem* 2016;20(1):203–13.
- [77] Pratap R, Singh B, Chandra S. Polymeric rechargeable solid-state proton battery. *J Power Sources* 2006;161:702–6.
- [78] Woo HJ, Liew C, Majid SR, Arof AK. Poly (ε-caprolactone)-based polymer electrolyte for electrical double-layer capacitors. *High Perform Polym* 2014;26:637–40, <http://dx.doi.org/10.1177/0954008314542168>.
- [79] Yusof YM, Majid NA, Kasmani RM, Illias HA, Kadir MFZ. The effect of plasticization on conductivity and other properties of starch/chitosan blend biopolymer electrolyte incorporated with ammonium iodide. *Mol Cryst Liq Cryst* 2014;1:73–88.
- [80] Liew CW, Ramesh S. Electrical, structural, thermal and electrochemical properties of corn starch-based biopolymer electrolytes. *Carbohydr Polym* 2015;124:222–8.

- [81] Winie T, Jamal A, Saaïd FI, Tseng T. Hexanoyl chitosan/ENR25 blend polymer electrolyte system for electrical double layer capacitor. *Polym Adv Technol* 2018;30:726–35, <http://dx.doi.org/10.1002/pat.4510>.
- [82] Kadir MFZ, Arof AK. Application of PVA–chitosan blend polymer electrolyte membrane in electrical double layer capacitor. *Mater Res Innov* 2013;15:217–20, <http://dx.doi.org/10.1179/143307511X13031890749299>.
- [83] Eftekhari A. On the mechanism of microporous carbon supercapacitors. *Mater Today Chem* 2018;7:1–4.
- [84] Eftekhari A. Surface diffusion and adsorption in supercapacitors. *ACS Sustain ChemEng* 2019;7:3692–701.
- [85] Eftekhari A. The mechanism of ultrafast supercapacitors. *J Mater Chem A Mater Energy Sustain* 2018;6:2866–76.
- [86] Teoh KH, Lim Chin-Shen, Liew Chiam-Wen, Ramesh S. Electric double-layer capacitors with corn starch-based biopolymer electrolytes incorporating silica as filler. *Ionics* 2015;21:2061–8.
- [87] Liew C, Ramesh S, Arof AK. Enhanced capacitance of EDLCs (electrical double layer capacitors) based on ionic liquid-added polymer electrolytes. *Energy* 2016;109:546–56, <http://dx.doi.org/10.1016/j.energy.2016.05.019>.
- [88] Subramaniam CK, Ramya CS, Ramya K. Performance of EDLCs using Nafion and Nafion composites as electrolyte. *J Appl Electrochem* 2011;41:197–206.
- [89] Shuhaimi NEA, Alias NA, Majid SR, Arof AK. Electrical double layer capacitor with proton conducting  $\kappa$ -carrageenan/chitosan electrolytes. *Funct Mater Lett* 2008;1:195, <http://dx.doi.org/10.1142/S1793604708000423>.
- [90] Shuhaimi NEA, Teo LP, Woo HJ, Majid SR, Arof AK. Electrical double-layer capacitors with plasticized polymer electrolyte based on methyl cellulose. *Polym Bull* 2012;69:807–26.
- [91] Kumar MS, Bhat DK. Polyvinyl alcohol-polystyrene sulphonic acid blend electrolyte for supercapacitor application. *Phys B* 2009;404:1143–7.
- [92] Selvakumar M, Bhat DK. LiClO<sub>4</sub> doped cellulose acetate as biodegradable polymer electrolyte for supercapacitors. *J Appl Polym Sci* 2008;110(1):594–602.
- [93] Shukur MF, Ithnin R, Kadir MFZ. Electrical characterization of corn starch–LiOAc electrolytes and application in electrochemical double layer capacitor. *Electrochim Acta* 2014;136:204–16.
- [94] Arof AK, Kufian MZ, Syukur MF, Aziz MF, Abdelrahman AE, Majid SR. Electrical double layer capacitor using poly(methyl methacrylate)–C4B08Li gel polymer electrolyte and carbonaceous material from shells of mata kucing (*Dimocarpus longan*) fruit. *Electrochim Acta* 2012;74:39–45.
- [95] Wei YZ, Fang B, Iwasa S, Kumagai M. A novel electrode material for electric double-layer capacitors. *J Power Source* 2005;141:386–91.
- [96] Aziz SB, Hamsan MH, Karim WO, Kadir MFZ, Brza MA, Abdullah OGH. High proton conducting polymer blend electrolytes based on chitosan: dextran with constant specific capacitance and energy density. *Biomolecules* 2019;9(7):267, <http://dx.doi.org/10.3390/biom9070267>.
- [97] Shujahadeen BA, Hamsan Muhamad H, Kadir Mohd FZ, Karim Wrya O, Abdullah Ranjdar M. Development of polymer blend electrolyte membranes based on chitosan: dextran with high ion transport properties for EDLC application. *Int J Mol Sci* 2019;20(13):3369, <http://dx.doi.org/10.3390/ijms20133369>.
- [98] Aziz SB, Hamsan MH, Abdullah RM, Kadir MFZ. A promising polymer blend electrolytes based on chitosan: methyl cellulose for EDLC application with high specific capacitance and energy density. *Molecules* 2019;24(13):2503, <http://dx.doi.org/10.3390/molecules24132503>.
- [99] Zhong C, Yida D, Hu W, Zhang J. A review of electrolyte materials and compositions for electrochemical supercapacitors. *Chem Soc Rev* 2015;44(21):7431–920.